

# A time-dependent scattering approach to core-level spectroscopies

Krissia Zawadzki,<sup>1</sup> Alberto Nocera,<sup>2</sup> and Adrian E. Feiguin<sup>1</sup>

<sup>1</sup>*Department of Physics, Northeastern University, Boston, Massachusetts 02115, USA*

<sup>2</sup>*Stewart Blusson Quantum Matter Institute, University of British Columbia, Vancouver, British Columbia V6T 1Z4, Canada*

(Dated: February 12, 2020)

While new light sources allow for unprecedented resolution in experiments with X-rays, a theoretical understanding of the scattering cross-section lacks closure. In the particular case of strongly correlated electron systems, numerical techniques are quite limited, since conventional approaches rely on calculating a response function (Kramers-Heisenberg formula) that is obtained from a time-dependent perturbative analysis of scattering processes. This requires a knowledge of a full set of eigenstates in order to account for all intermediate processes away from equilibrium, limiting the applicability to small tractable systems. In this work, we present an alternative paradigm allowing to explicitly solving the time-dependent Schrödinger equation without the limitations of perturbation theory, a faithful simulation of all scattering processes taking place in actual experiments. We introduce the formalism and an application to Mott insulating Hubbard chains using the time-dependent density matrix renormalization group method, which does not require a priori knowledge of the eigenstates and thus, can be applied to very large systems with dozens of orbitals. Away from the ultra short lifetime limit we find signatures of spectral weight at low energies that can be explained in terms of gapless multi-spinon excitations. Our approach can readily be applied to systems out of equilibrium without modification.

## I. INTRODUCTION

In the past couple of decades, advances in experiments with light have paved the way to a new era in the study of elementary excitations of correlated matter[1–5]. High intensity X-ray sources, ultrafast pulses, and detectors with enhanced resolution for photon scattering measurements[1, 4, 6] have driven a continuous improvement of techniques such as X-ray absorption (XAS) and emission (XES) spectroscopies [7–9], resonant inelastic X-ray scattering (RIXS) [1, 4, 6, 10] as well as their corresponding dynamical versions (e.g. non-equilibrium or NE-XAS and time-resolved tr-RIXS). In particular, the possibility to probe with energy and momentum resolution excitations arising from charge, spin and orbital degrees of freedom has made RIXS the favorite tool to study the spectrum of solids and complex materials, including transition-metal compounds [11–15], Mott and anti-ferromagnetic insulators and unconventional high  $T_c$  superconductors [16–19].

This fruitful period has also been marked by theoretical efforts to understand more in depth the scattering processes and the nature of the dynamical correlation functions probed by these experiments[1]. In this respect, uncovering various aspects underlying the excitation spectrum of a system is associated to the calculation of dynamical correlation functions, a task that, to date, remains challenging. The limitations of available techniques to compute spectral properties in strongly correlated systems has curbed further theoretical progress [20]. For instance, the Bethe Ansatz [21] and Dynamical Mean-Field Theory (DMFT) [22] are restricted to relatively simple model Hamiltonians, whereas time-dependent Density Functional Theory (TD-DFT) [8] covers weakly coupled regimes. Exact diagonalization (ED), which has been the most employed numerical tool

to calculate of the spectrum of solids and complex materials [10–14, 23–37], provides access to small clusters and limits the momentum resolution.

The main limiting factor in these calculations is that core hole spectroscopies such as RIXS involve intermediate processes that can only be accounted for by knowing explicitly all the eigenstates of the system, requiring a full diagonalization of the Hamiltonian. Very recently, Nocera *et al.* introduced a novel framework [38] based on the dynamical density matrix renormalization group (dDMRG)[39–41] aiming at extending the range of RIXS (and XAS) computations to systems beyond the reach of exact diagonalization (ED). Even though cluster sizes much bigger than ED were reached, the algorithm proposed in ref. 38 requires a number of DMRG simulations scaling linearly in the size of the system, making the computation of the entire RIXS spectrum a difficult task for challenging Hamiltonians.

In this work, we propose an alternative approach in which the calculation of spectrum is recast as a scattering problem that can be readily solved by means the time-dependent DMRG method in a framework that does not require a full set of eigenstates of the Hamiltonian of the system. This powerful formulation overcomes all the hurdles imposed by previous methods that rely on explicitly obtaining dynamical spectral functions by means of generalized Fermi golden rules (Kramer’s-Heisenberg). The paper is organized as follows: Sec. II recaps the principles of light-matter interactions taking place in X-ray experiments, presenting the analytical form of the scattering amplitudes probed in XAS (subsec. II A) and direct RIXS (subsec. II B). With this foundation, we then introduce our approach and show how to recast the calculation of the spectrum as a time-dependent scattering problem with applications to XAS in subsec. III A and RIXS, subsec. III B. In Sec. III we describe the im-

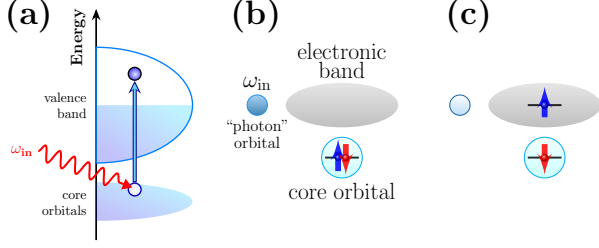


FIG. 1. Schematic representation of an X-ray absorption process, in which an incident photon excites a core electron into the valence band, leaving a hole behind (a). Panel (b) represents an the initial state and (c), the final configuration after the photon has created the excitation. A Coulomb interaction ensues between the empty orbital and the band electrons.

plementation of our proposal in the tDMRG framework, presenting results for a one-dimensional Mott insulator described by a Hubbard chain, a model which has been widely used to simulate XAS and RIXS in cuprates. Finally, we discuss our findings and implications in Sec.V.

## II. LIGHT-MATTER INTERACTIONS

We hereby briefly review the basic ideas that describe an X-ray scattering experiment and provide a theoretical background to put the problem in context. Since X-rays are a highly energetic beam of photons, we represent them through a vector potential:

$$\mathbf{A}(\mathbf{r}) = \sum_{\mathbf{k}, \lambda} A_{\mathbf{k}} \mathbf{e}_{\mathbf{k}\lambda} (b_{\mathbf{k}\lambda} e^{i\mathbf{k}\mathbf{r}} + b_{\mathbf{k}\lambda}^{\dagger} e^{-i\mathbf{k}\mathbf{r}}),$$

where  $A_{\mathbf{k}} = \sqrt{2\pi c^2 / V_s \omega_{\mathbf{k}}}$  is the normalized amplitude in volume  $V_s$ , with  $\omega_{\mathbf{k}} = c|\mathbf{k}|$ . The polarization unit vectors  $\mathbf{e}_{\mathbf{k}\lambda}$  ( $\lambda=1,2$ ) point in directions perpendicular to the propagation of the photons with momentum  $\mathbf{k}$ , represented by the conventional bosonic creation and annihilation operators  $b^{\dagger}$ ,  $b$ . The full Hamiltonian including the solid and the radiation field is written as

$$H = H_0 + H_{ph} + V, \quad (1)$$

where  $H_0$  describes the electrons and nuclei in the solid, and  $H_{ph} = \sum_{\mathbf{k}, \lambda} \omega_{\mathbf{k}} (b_{\mathbf{k}, \lambda}^{\dagger} b_{\mathbf{k}, \lambda} + 1/2)$ . The light-matter interaction is given by

$$V = \frac{e}{mc} \sum_i \mathbf{p}_i \cdot \mathbf{A}(\mathbf{r}_i) + \frac{e}{2mc} \sum_i \sigma_i \cdot \nabla \times \mathbf{A}(\mathbf{r}_i), \quad (2)$$

where the first term accounts for the interaction of the electric field with the momentum  $\mathbf{p}$  of the electrons and the second term describes the magnetic field acting on the electron spin  $\sigma$ . In the following, we will ignore the magnetic interaction as well as higher order terms that are not included in this expression. In this case, by replacing the quantized vector operator into this expression, we

obtain:

$$V = \frac{e}{mc} \sum_i \sum_{\mathbf{k}, \lambda} A_{\mathbf{k}} (b_{\mathbf{k}, \lambda}^{\dagger} \mathbf{e}_{\mathbf{k}, \lambda} \cdot \mathbf{p}_i e^{i\mathbf{k}\mathbf{R}_i} + \text{h.c.}) \quad (3)$$

$$= \sum_{\mathbf{k}, \lambda} (b_{\mathbf{k}, \lambda}^{\dagger} D_{\mathbf{k}, \lambda} + \text{h.c.}) \quad (4)$$

where we have assumed the dipole limit in which  $e^{i\mathbf{k}\cdot\mathbf{r}} \simeq e^{i\mathbf{k}\cdot\mathbf{R}_i}$  where  $\mathbf{R}_i$  is the position of the ion to which electron  $i$  is bound, and we have introduced the dipole operator

$$D_{\mathbf{k}, \lambda} = \sum_i \frac{e}{mc} A_{\mathbf{k}} \mathbf{e}_{\mathbf{k}, \lambda} \cdot \mathbf{p}_i e^{i\mathbf{k}\cdot\mathbf{R}_i}. \quad (5)$$

We start our discussion by first considering a scattering process in which a photon with momentum  $\mathbf{k}$ , energy  $\omega_{\mathbf{k}}$  and polarization  $\mathbf{e}_{\mathbf{k}, \lambda}$  is absorbed, leaving the system energetically excited. The possible final states will be determined by the allowed dipolar transitions. In particular, one finds:

$$\langle n' l' m' | \mathbf{p}_i | n l m \rangle \neq 0 \iff \Delta l = \pm 1 \text{ and } \Delta m = 0, \pm 1$$

where  $\Delta l = l' - l$  and  $\Delta m = m' - m$ , and  $l$  represents the orbital angular momentum with projection  $m$ . In the process we are interested in, this operator will create a core-hole excitation. In particular, we focus on the Cu  $L$ -edge ( $2p \rightarrow 3d$ ) transition in a typical X-ray scattering experiment on a transition metal oxide cuprate material[42]. In this case,

$$D_{\mathbf{k}, \lambda} = \sum_{i, \sigma, \alpha} (e^{i\mathbf{k}\cdot\mathbf{R}_i} \Gamma_{\alpha}^{\lambda} d_{i, \sigma}^{\dagger} p_{i, \alpha, \sigma} + \text{h.c.}), \quad (6)$$

where  $d^{\dagger}$  adds an electron to the valence band ( $3d_{x^2-y^2}$ ) and  $p_{\alpha}$  creates a hole in a  $2p_{\alpha}$  orbital. The coefficients  $\Gamma_{\alpha}^{\lambda}$  are determined by the matrix elements of the dipole operator,  $\Gamma_{\alpha}^{\lambda} \propto \langle 2p_{\alpha} | \mathbf{e}_{\mathbf{k}, \lambda} \cdot \mathbf{r} | 3d_{x^2-y^2} \rangle = 1$ , where we have expressed the dipole operator in terms of the position operator  $\mathbf{r}$ [1]. It is typically assumed that the core hole is strongly localized and only one Cu  $2p_{\alpha}$  orbital is involved in the process.

After the excitation is created, the conduction electrons will experience a local Coulomb potential  $-U_c$  in the presence of the core hole and Hamiltonian (1) is modified accordingly:

$$\begin{aligned} H &= H_0 + H_c + H_{ph}, \quad H_c = -U_c \sum_i n_{di} (1 - n_{pi}), \\ V &= V_{in} + V_{out}, \quad V_{out} = V_{in}^{\dagger} \\ V_{in} &= \sum_{\mathbf{k}, \lambda} b_{\mathbf{k}, \lambda} D_{\mathbf{k}, \lambda} = \sum_{\mathbf{k}, \lambda} b_{\mathbf{k}, \lambda} \sum_i (e^{i\mathbf{k}\cdot\mathbf{R}_i} D_{i, \lambda}^{\dagger} + \text{h.c.}), \end{aligned} \quad (7)$$

with  $D_{i, \lambda}^{\dagger} = \sum_{\alpha, \sigma} \Gamma_{\alpha}^{\lambda} d_{i, \sigma}^{\dagger} p_{i, \alpha, \sigma}$  and  $n_p = \sum_{\sigma} p_{\sigma}^{\dagger} p_{\sigma}$ , and it is important to notice that the  $p$  orbital can only be double or single occupied, but never empty since that would imply a two photon process.

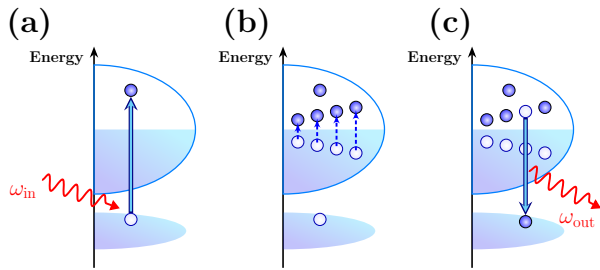


FIG. 2. In a RIXS experiment, a core electron is excited into the valence band (a). After some time, an electron decays back into the core orbital, emitting a photon and leaving the system in an excited state, (b) and (c).

Due to the large local spin-orbit coupling in the core  $2p$  orbital (of the order of  $20eV$  at the Cu L-edge) the  $2p$  orbitals split by their total angular momentum  $j$  and  $j_z$ , the projection along the  $z$  axis, corresponding to the  $L_2$  ( $\tilde{j} = 1/2$ ) and  $L_3$  ( $\tilde{j} = 3/2$ ) transition edges. Because the energy separation between the two resonances is much larger than the core-hole lifetime broadening, we neglect the possibility of interference between the two edges, such that we have either  $D_{\mathbf{k},\lambda} \simeq D_{\mathbf{k},\lambda,\tilde{j}=1/2}$  or  $D_{\mathbf{k},\lambda} \simeq D_{\mathbf{k},\lambda,\tilde{j}=3/2}$ . As a consequence, neither the spin nor the orbital angular momentum of the  $2p$  band are good quantum numbers in the scattering process, but only the total angular momentum is conserved, allowing for orbital and spin “flip” processes at the Cu-L edge RIXS[10, 42]. We shall elaborate on this below.

### A. X-ray absorption

We now derive the X-ray absorption spectrum (XAS), which describes the aforementioned situation. This is a single photon process, in which an electron is transferred from the core orbital into a partially filled or empty band. Therefore, it is identified with the empty density of states, with corrections introduced by the presence of the core potential that allow one to extract the binding energy of the electron-hole pairs (See schematic process in Fig.1).

The calculation of the transition amplitudes is a simple exercise of time-dependent perturbation theory. We assume that initially system and photons are decoupled and the electrons are in the ground state  $|0\rangle$  with energy  $E_0$ , such that the terms in  $V$  become the perturbation. The final states  $|f\rangle$  contain an excited electron,

a core hole and one less photon in the radiation field. At time  $t = 0$ , the total wave-function of the electrons plus photons is a product state  $|\psi\rangle = |0\rangle \otimes |\phi\rangle$ . Since we are interested in a single photon absorption process, it suffices to consider a photon bath  $|\phi\rangle$  initially consisting of one photon in mode  $\mathbf{k}$  with energy  $\omega_{\mathbf{k}}$ . The XAS spectrum will be determined by the probability of the system absorbing the photon with energy  $\omega_{\mathbf{k}}$  at time  $t$ ,  $I_{XAS}(\omega_{\mathbf{k}}, t) = \langle \psi | b_{\mathbf{k}}^\dagger b_{\mathbf{k}} | \psi \rangle - \langle t | b_{\mathbf{k}}^\dagger b_{\mathbf{k}} | t \rangle = 1 - \langle t | b_{\mathbf{k}}^\dagger b_{\mathbf{k}} | t \rangle$ , where  $|t\rangle = U(t, 0)|\psi\rangle$  and  $U(t, t') = T \exp -i \int_{t'}^t H(\tau) d\tau$  is the evolution operator. Since the ground state has no core-hole, it cannot decay and emit a photon. We ignore the polarization index  $\lambda$  from now on. The first order contribution is given by:

$$I_{XAS}(\omega_{\mathbf{k}}, t) = \int_0^t dt_1 \int_0^{t_1} dt_2 \langle V_{out}(t_1) | b_{\mathbf{k}}^\dagger b_{\mathbf{k}} | V_{in}(t_2) \rangle$$

In the large  $t$  limit this becomes:

$$I_{XAS}(\omega_{\mathbf{k}}) = 2\pi N \sum_f |\langle f | D_0 | 0 \rangle|^2 \delta(\omega_{\mathbf{k}} - E_f + E_0), \quad (8)$$

which is simply Fermi’s golden rule, the sum in  $f$  runs over a complete set of eigenstates  $|f\rangle$  in the presence of a core-hole. Note that the operator  $D_0$  is measured only at one atomic site due to translational invariance. This implies that the formulation can actually be reduced to a single site scattering problem.

### B. Resonant Inelastic X-ray Scattering

Resonant inelastic X-ray scattering (RIXS) is a higher order process that can be described as a combination of XAS and X-ray emission spectroscopy (XES), in which the system absorbs a photon with energy  $\omega_{in}$  and emits another one with energy  $\omega_{out}$  (we focus on the so-called “direct RIXS” processes, see Fig.2 and Fig. 1 in Ref.12). As a consequence, the photon loses energy and the electrons in the solid end up in an excited state with momentum  $\mathbf{k}' - \mathbf{k}$  and energy  $\Delta\omega = \omega_{out} - \omega_{in}$ . While in principle the resulting spectrum is a function of two frequencies, the incident photon  $\omega_{in}$  is tuned to match one of the absorption edges, hence the resonant nature of the process. Employing similar arguments as in the previous section, the final response is determined by measuring the final occupation of the  $\omega_{out}$  mode. However, the spectrum is determined by the second order correction (we ignore spin indices for now):

$$\begin{aligned} I_{RIXS}(\omega_{out}, t) &= \int_0^t dt_1 \int_0^{t_1} dt_2 \int_0^{t_2} dt_1' \int_0^{t_1'} dt_2' \langle V_{out}(t_1') V_{in}(t_2') b_{\mathbf{k}'}^\dagger b_{\mathbf{k}} V_{out}(t_2) V_{in}(t_1) \rangle \\ &= \int_0^t dt_2 \int_0^{t_2} dt_1 \int_0^{t_1} dt_2' \int_0^{t_2'} dt_1' e^{i(\omega_{in} + E_0)(t_1' - t_1)} \langle V_{out} e^{iH(t_2' - t_1')} V_{in} e^{-iH t_2'} b_{\mathbf{k}'}^\dagger b_{\mathbf{k}} e^{iH t_2} V_{out} e^{-iH(t_2 - t_1)} V_{in} \rangle \end{aligned}$$

$$\rightarrow 4\pi^2 \sum_f \left| \sum_n \frac{\langle f|D_{\mathbf{k}'}|n\rangle \langle n|D_{\mathbf{k}}|0\rangle}{(\omega + E_0 - E_n + i\eta)} \right|^2 \delta(\omega_{in} - \omega_{out} + E_0 - E_f), \quad (9)$$

where we have taken the large  $t$  limit in the last step. In this expression, the eigenstates  $|n\rangle$  belong to the intermediate Hamiltonian in the presence of the core-hole potential, while the eigenstates  $|f\rangle$  are a full basis of the unperturbed electronic Hamiltonian without the core-hole (notice that the Hamiltonian  $H_0$  does not include a hybridization between  $p$  and  $d$  orbitals, hence the particle numbers  $N_p$  and  $N_d$  are conserved quantities). We observe that the energy difference  $\Delta\omega = \omega_{out} - \omega_{in} = E_f - E_0$  is transferred to the electrons in the band. Therefore, the energy lost by the photon is pumped into the system. In the absence of spin-orbit coupling, the states  $|f\rangle$  will have the same spin and particle number as the ground state, hence they can represent a particle-hole excitation, or a spin excitation with an even number of spin flips such that  $\Delta S^z = 0$ . On the other hand, the spin-orbit interaction can introduce spin-flip processes as depicted in Fig. 3. These can result in the electronic band having a final state with a total spin different than the initial one,  $\Delta S^z = \pm 1$ . In this case, the RIXS spectrum will reflect both neutral particle-hole excitations and spin excitations with an odd number of spin flips.

We finally point out that, in order to account for the finite lifetime  $\eta$  of the electron-hole pair, a real damping phase  $\exp(-\eta\Delta t)$  is conventionally added to the evolution operator between the occurrences of  $V_{in}$  and  $V_{out}$ , that translates into an artificial broadening of the spectrum that mimics the finite duration of the core-hole lifetime. In the sections below we proceed to elaborate on these aspects of the problem and expand the discussion.

### III. TIME-DEPENDENT SCATTERING APPROACH

The numerical calculation of the RIXS spectrum is computationally very costly, since it requires a knowledge of a full set of eigenstates of the Hamiltonian  $|n\rangle$  and  $|f\rangle$  that appear in Eq. (9). Therefore, it can only be carried out in particular manageable situations, such as the case of non-interacting systems, or interacting problems with few degrees of freedom and/or small system sizes. We can simply overcome these limitations by recognizing that the problem involves single photon processes and can be recast as a scattering problem that can be readily solved in the time domain. As seen before, the spectra can be obtained directly by measuring the occupation of certain states after some (photon in/photon out) tunneling event. For illustration purposes, we start with XAS, and generalize the formulation to RIXS in the following section.

#### A. XAS

In order to progressively introduce the numerical formalism, we start as before with a description of XAS. Since the absorption process involves only one photon, we simply consider a single photon orbital at energy  $\omega_{in}$  that is initially occupied. We include a single localized core orbital at position “0” that is initially double occupied. The Hamiltonian of the problem is now defined as

$$H = H_0 + H_c + \omega_{in}n_b, \quad V_{in} = \Gamma b \sum_{\sigma} d_{0\sigma}^{\dagger} p_{0\sigma},$$

$$H_c = -U_c \sum_{\sigma} (1 - n_{p0\sigma})n_{d0}, \quad (10)$$

where  $b$  represents the only photon participating in the problem.

In order to measure the absorption spectrum, we simply calculate the occupation of the photon orbital  $n_b = b^{\dagger}b$  as a function of time. In the perturbative limit in the coupling  $\Gamma$ , our time-dependent scattering approach is equivalent to the standard approach to XAS:

$$I_{XAS}(\omega_{in}, t) = \langle n_b(t) \rangle$$

$$= 8\Gamma^2 \sum_f |\langle f|V_{in}|0\rangle|^2 \frac{\sin^2((\omega_{in} - (E_f - E_0))t/2)}{(\omega_{in} - (E_f - E_0))^2}. \quad (11)$$

This expression approaches a delta function in the large  $t$  limit. However, this limit can never be reached since after certain time, an electron may recombine with the core-hole *i.e.*, tunnel back into the core-orbital (which is the same as the photon tunneling back into the photon orbital). The tunneling time will be determined by the amplitude of the coupling  $\Gamma$ , and it will be inversely proportional to the linewidth in the spectrum, a manifestation of the uncertainty principle. As a consequence, practical simulations are conducted up to a time  $t_{max}$  smaller than the characteristic “time of passage” [43]. Notice that this is basically equivalent to the artificial frequency broadening introduced in the calculation of spectral functions, so it cannot be considered an issue, but a feature of the approach. In ultrafast experiments, the “infinite time” limit that yields a delta in Fermi’s golden rule is never reached nonetheless, giving a natural broadening to the spectral features. As can be observed by direct inspection, both expressions (8) and (11) are completely equivalent, but the latter will be carried out using an exact time-dependent simulation, as described in section IV.

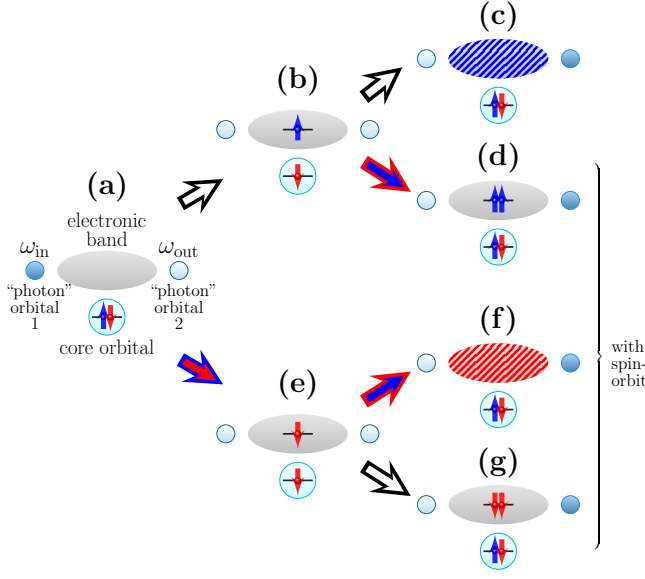


FIG. 3. Depiction of the possible processes accounted for by our formulation of the direct RIXS problem: The incident photon has energy  $\omega_{in}$ , and the “detector” is tuned to a target energy  $\omega_{out}$ . The (b)→(c) path represents a process without spin orbit in which the final state of the band has the same quantum numbers as the original one. The (e) path corresponds to a spin-flip after absorption, while (d) and (f) undergo a spin-flip after emission. The final state can reverse the spin flip (d),(g) or leave the band with a different spin (c),(f). There is a similar cascade of processes related to these by time-reversal.

## B. RIXS

Same as discussed in the section above, RIXS can be formulated in terms of a single photon being absorbed or

$$\begin{aligned}
 I_{RIXS}(\omega_{in}, \omega_{out}, t) &= \sum_{\sigma\sigma'\sigma''} \sum_{\tau\tau'\tau''} \int_0^t dt_2 \int_0^{t_2} dt_1 \int_0^t dt_2' \int_0^{t_2'} dt_1' \langle \psi(t) | n_{b,d} | \psi(t) \rangle \\
 &= \sum_{\sigma\sigma'} \sum_{\tau\tau'} \sum_{\sigma'',\tau''} (\Gamma_s^{\tau''\tau} \Gamma_d^{\tau''\tau'} \Gamma_d^{\sigma''\sigma'} \Gamma_s^{\sigma''\sigma}) I_{RIXS}^{\tau\tau',\sigma'\sigma}
 \end{aligned} \tag{13}$$

where

$$I_{RIXS}^{\tau\tau',\sigma'\sigma} = \int_0^t dt_2 \int_0^{t_2} dt_1 \int_0^t dt_2' \int_0^{t_2'} dt_1' e^{i(\omega_{in} + E_0)(t_1' - t_1)} \langle \phi_0 | d_{0\tau} e^{iH_c'(t_2' - t_1')} d_{0\tau'}^\dagger e^{-iH_0(t_2' - t_2)} d_{0\sigma'} e^{-iH_c'(t_2 - t_1)} d_{0\sigma}^\dagger | \phi_0 \rangle.$$

where  $H_c' = H_0 - U_c n_{d0}$  and  $|\phi_0\rangle$  is the initial state of the electronic bands. In this expression  $n_{b,d}$  kills all contributions of terms in  $V_{out}$  that leave a photon on the source: only combinations that leave the detector with a photon in the same final and the core orbital double occupied state will survive. Using the fact that the initial state

emitted by the system. This time, we consider the system locally connected to two photon orbitals, one with energy  $\omega_{in}$  that will serve as the “source” for absorption, and a second one with energy  $\omega_{out}$  will be the “detector” for emission and is initially empty. For the time being, we will describe a local problem in which both photons only interact with electrons at a single site “0”. The problem is described by the Hamiltonian:

$$\begin{aligned}
 H &= H_0 + H_c + \omega_{in} n_{b,s} + \omega_{out} n_{b,d} + V, \\
 V &= V_{in} + V_{out}; \quad V_{out} = V_{in}^\dagger, \\
 V_{in} &= \sum_{\sigma,\sigma'=\uparrow,\downarrow} V_{in}^{\sigma\sigma'} \\
 V_{in}^{\sigma\sigma'} &= (\Gamma_s^{\sigma\sigma'} b_s + \Gamma_d^{\sigma\sigma'} b_d) d_{0\sigma'}^\dagger p_{0\sigma}, \\
 H_c &= -U_c \sum_{\sigma} (1 - n_{p0\sigma}) n_{d0},
 \end{aligned} \tag{12}$$

where we have introduced couplings  $\Gamma_i^{\sigma\sigma'}$  that can be turned on and off selectively depending of the case of interest, as we describe below. For instance, in the absence of spin-orbit interaction, only  $\Gamma_i^{\sigma\sigma}$  will be non-zero. Otherwise, the spin projection is no longer a good quantum number and the core-electron is allowed to flip spin when it is excited.

We observe that since there is only one photon at play, only one core-electron will be excited at most at any given time. The goal is to measure the occupation of the detector  $\langle \psi(t) | n_{b,d} | \psi(t) \rangle$  after the scattering term is turned on, starting from an initial state where the core orbital is double occupied and the source has a photon while the detector is empty (see Fig.3). While we carry out exact numerical simulations of the full non-equilibrium problem, one can show that our time-dependent scattering approach is equivalent to the standard RIXS response based on the Kramers-Heisenberg formula in the perturbative limit. The the second order contribution is proportional to:

is a product state, we can trace out the core orbital and the photons, obtaining an expression that only depends on the band electrons. The resulting contributions can be split into spin conserving and non-conserving ones:

$$I_{RIXS}^{\Delta S=0} = 2 \sum_{\sigma\tau} \Gamma_s^{\uparrow\tau} \Gamma_d^{\uparrow\tau} \Gamma_d^{\uparrow\sigma} \Gamma_s^{\uparrow\sigma} I_{RIXS}^{\uparrow\uparrow,\uparrow\uparrow} +$$

$$+ 2 \sum_{\sigma\tau} \Gamma_s^{\uparrow\tau} \Gamma_d^{\uparrow\tau} \Gamma_d^{\downarrow\sigma} \Gamma_s^{\downarrow\sigma} I_{RIXS}^{\uparrow\uparrow,\downarrow\downarrow} \quad (14)$$

$$I_{RIXS}^{\Delta S=1} = 2 \sum_{\sigma\tau} \Gamma_s^{\downarrow\tau} \Gamma_d^{\uparrow\tau} \Gamma_d^{\uparrow\sigma} \Gamma_s^{\downarrow\sigma} I_{RIXS}^{\downarrow\uparrow,\uparrow\downarrow}, \quad (15)$$

where we have used  $I_{RIXS}^{\uparrow\uparrow,\uparrow\uparrow} = I_{RIXS}^{\downarrow\downarrow,\downarrow\downarrow}$ ,  $I_{RIXS}^{\uparrow\uparrow,\downarrow\downarrow} = I_{RIXS}^{\downarrow\downarrow,\uparrow\uparrow}$  and  $I_{RIXS}^{\downarrow\uparrow,\uparrow\downarrow} = I_{RIXS}^{\uparrow\downarrow,\downarrow\uparrow}$ . By turning the couplings  $\Gamma$  on and off, this protocol allows us to measure each of the terms individually, including the interference contribution (second term in (14)) and spin-orbit contribution, Eq.(15). Explicitly, we proceed by carrying out a time-dependent simulation with a photon in the source orbital, and the drain empty. By setting  $\Gamma_s^{\sigma\sigma'} = \Gamma_d^{\tau\tau'} = \Gamma$ , and all others set to zero, to obtain a wave-function  $|\psi_{\sigma\sigma',\tau\tau'}(t)\rangle$ . The different terms are given by:

$$\langle \psi_{\uparrow\uparrow,\uparrow\uparrow} | n_{b,d} | \psi_{\uparrow\uparrow,\uparrow\uparrow} \rangle = \Gamma^4 I_{RIXS}^{\uparrow\uparrow,\uparrow\uparrow} \quad (16)$$

$$\langle \psi_{\downarrow\downarrow,\downarrow\downarrow} | n_{b,d} | \psi_{\uparrow\uparrow,\uparrow\uparrow} \rangle = \Gamma^4 I_{RIXS}^{\downarrow\downarrow,\uparrow\uparrow} \quad (17)$$

$$\langle \psi_{\uparrow\uparrow,\uparrow\downarrow} | n_{b,d} | \psi_{\uparrow\uparrow,\uparrow\downarrow} \rangle = \Gamma^4 I_{RIXS}^{\uparrow\downarrow,\uparrow\downarrow}. \quad (18)$$

To account for all the contributions, a total of four independent calculations would be required, because the interference term (17) is an expectation value with two different wave-functions. Note, however, that setting all the  $\Gamma_s^{\sigma,\sigma'} = \Gamma_d^{\sigma,\sigma'} = \Gamma$  will yield the total RIXS spectrum automatically from a single time-dependent simulation. The full calculation proceeds as follows: the energy  $\omega_{in}$  is set to the transition edge and tDMRG simulations are carried out in parallel for each value of  $\omega_{out}$ . The full spectrum is obtained by measuring the occupation of the detector at time  $t_{probe}$ . Details are described in the following section.

## IV. RESULTS

We hereby demonstrate how to implement these protocols using the time-dependent density matrix renormalization group method (tDMRG) [44–47]. We will describe the  $d$  band by means of the Hubbard model in one-dimension with open boundary conditions:

$$H = -J \sum_{i=1,\sigma}^L \left( d_{i\sigma}^\dagger d_{i+1\sigma} + \text{h.c.} \right) + U \sum_{i=1}^L n_{di\uparrow} n_{di\downarrow} \quad (19)$$

Here,  $d_{i\sigma}^\dagger$  creates an electron of spin  $\sigma$  on the  $i^{\text{th}}$  site along a chain of length  $L$ . The on-site Coulomb repulsion is parametrized by  $U$ , respectively. We express all energies in units of the hopping parameter  $J$  (the symbol “ $t$ ” will be reserved to represent time, which will be expressed in units of  $1/J$ ). We consider a half-filled band describing a one-dimensional Mott insulator, and measure the local spectra by connecting source and drain to a site at the center of the chain.

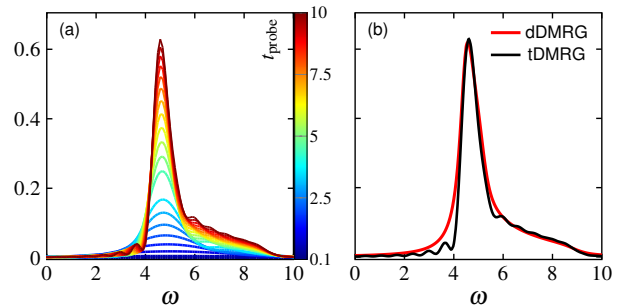


FIG. 4. XAS results using a time-dependent scattering approach for a Mott insulating Hubbard chain with  $L = 64$ ,  $U = 8$  and  $U_c = 1.5$ . (a) Evolution of the spectrum with the measuring time  $t_{probe}$ ; (b) Comparison with DDMRG results.

### A. XAS spectrum

We simulated a Mott insulating Hubbard chain of length  $L = 64$ , with  $N = L$  electrons,  $U = 8$ ,  $U_c = 1.5$  and evolved in time up to  $t = 15$  using  $m = 200$  DMRG states and time steps  $\delta t = 0.1$ , which yields a truncation error smaller than  $10^{-7}$ . In all the calculations shown below, unless otherwise specified, we chose the dipole coupling  $\Gamma = 0.2$ . Results are shown in Fig.4. The transition edge is at  $E'_0(N+1) - E_0(N)$ , where  $E'_0$  and  $E_0$  are the ground state energies with and without the localized core-hole potential, respectively. Panel (a) shows the evolution of the spectrum in time. As expected, longer times translate into improved resolution in energy. Panel (b) shows a comparison with dynamical DMRG data and we observe excellent agreement between both approaches.

### B. RIXS spectrum

We followed a similar prescription to obtain the full RIXS spectrum for the Mott insulating Hubbard chain. Results obtained using the time-dependent scattering approach with  $m = 300$  DMRG states are shown in Fig.5, compared to data obtained with dynamical DMRG for the same system size and  $m = 800$  states. The overall agreement is qualitatively very good, but the DDMRG results clearly suffer from poor precision particularly at high energies. The discrepancies can be attributed to the fact that the time-evolved wave-function contains contributions of higher-order. For instance, cases in which a photon ends into the detector after bouncing back and forth at the source, or undergoing intermediate non-radiative processes.

The resulting spectrum contains signatures of a broad high-energy band, and a narrower low energy band with higher concentrated weight. One would think that the low energy signal originates from elastic scattering, but this contribution is at zero energy, as can be seen clearly in panel (b) of the figure. In addition, the elastic contribution has been removed from the DDMRG data, im-

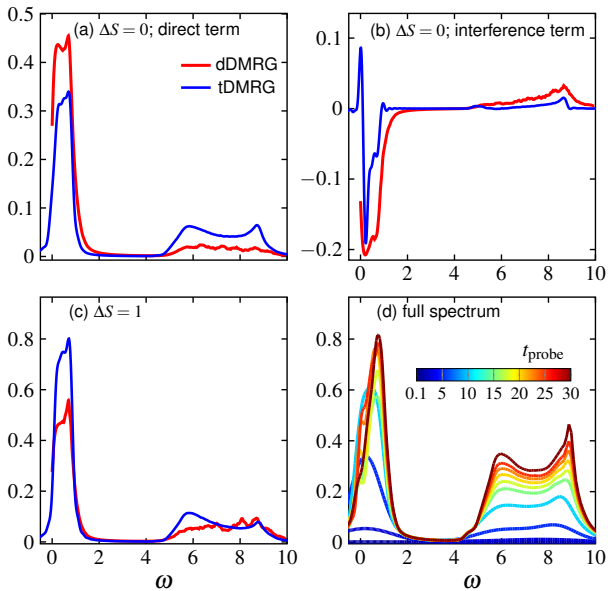


FIG. 5. RIXS results using a time-dependent scattering approach for a Mott insulating Hubbard chain with  $U = 8$  and  $U_c = 1.5$  and  $L = 64$  sites. Panels show (a) the direct contribution, (b) interference term, (c) spin-flip term, and (d) full spectrum, also following its evolution as a function of time. DDMRG results are also shown for comparison.

plying that this low energy band indeed corresponds to spectral weight *in the gap*. While this can be confusing, it is readily explained in terms of multi spinon excitations with an even number of spin-flips[21]. While a Mott insulator has a charge gap, the spin excitations are gapless, a manifestation of spin-charge separation in one spatial dimension. Clearly, there are no available states within the Mott gap. The high energy features correspond to holon-doublon excitations that transfer spectral weight from the lower into the upper Hubbard band.

### 1. Core-hole lifetime and dependence of the lineshape

The RIXS spectrum is usually interpreted by means of the “ultra-short lifetime expansion” (UCL) [10, 12, 48], that assumes that the lifetime of the core-hole is practically zero. In this limit, it has been shown that, at least in the case of Cu-L edge for cuprates[10], the RIXS contributions to the spectrum can be associated to collective density (for  $\Delta S = 0$ ) and spin (for  $\Delta S = 1$ ) excitations described by simpler two-point spectral functions

$$I_{RIXS}^{\Delta S=0} \sim \sum_f |\langle f | \tilde{n}_0 | 0 \rangle|^2 \delta(\omega - E_f + E_0)$$

$$I_{RIXS}^{\Delta S=1} \sim \sum_f |\langle f | S_0^z | 0 \rangle|^2 \delta(\omega - E_f + E_0). \quad (20)$$

For  $\Delta S = 0$ , it is important to notice that the RIXS response reduces to a generalized density spectral function,

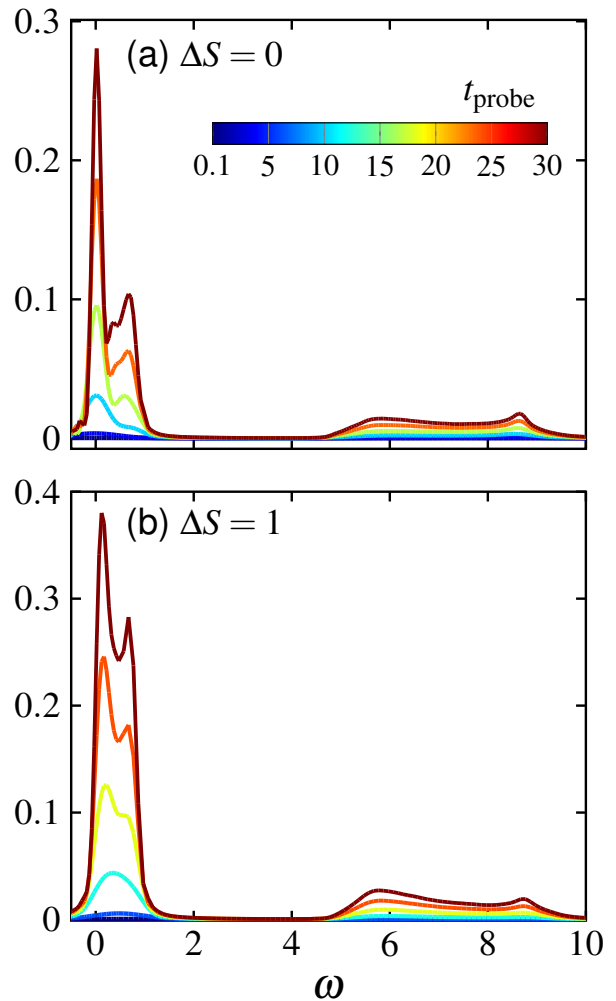


FIG. 6. (a) Spin conserving and (b) non-conserving RIXS channels for a Mott insulating Hubbard chain with  $U = 8$ ,  $U_c = 1.5$ ,  $\Gamma = 0.1$ ,  $L = 64$  sites, for different probing times  $t_{probe}$ . The inelastic features at low energies emerge after a characteristic time for the electrons to break and decay into spinons and doublons.

where  $\tilde{n}_0 = \sum_\sigma \tilde{n}_{0,\sigma}$ , with  $\tilde{n}_{0,\sigma} = c_{0,\sigma}^\dagger (1 - n_{0,\bar{\sigma}}) c_{0,\sigma}$ . To highlight this feature we report the *direct* ( $I_{RIXS}^{\uparrow\uparrow,\uparrow\uparrow}$ ) and *interference* components ( $I_{RIXS}^{\uparrow\uparrow,\downarrow\downarrow}$ ) of the RIXS spectrum in Fig. 5(a) and Fig. 5(b), respectively. Since the system is a Mott insulator, the *standard* density spectral function is gapped[49], while the  $I_{RIXS}^{\Delta S=0}$  response can be gapless, according to our observations in Fig. 5. We interpret these low energy excitations inside the Mott gap as spin excitations with  $\Delta S_z = 0$  produced by even number of spin flips and not changing the number of electrons  $N$ . This is a unique feature of RIXS, in that these spectral features are observable as long as the core-hole lifetime is very short but nonzero.

The core-hole lifetime is controlled by non-radiative decay mechanisms due to electronic correlations, such as Auger, and radiative decay, directly related to the magni-

tude of the dipolar coupling  $\Gamma$ . In a Mott insulator away from equilibrium one can imagine high-order processes in which an electron in the band decays into the core orbital, simultaneously creating a particle hole excitation with an additional doublon in the upper Hubbard band. The decay of the doublon into spinons is unlikely due to the weak spinon dispersion and the vanishing coupling between charge and spin [50–52] (long doublon lifetime has also been observed in higher dimensions [53–56]). In our calculations, the lineshape will be determined by the time lapsing between the moment the photon source is turned on, and the emitted photon is measured by the detector, our  $t_{probe}$ . In Fig. 6 we show results for the spin conserving and non-conserving channels as a function of the probing time. The UCL limit would correspond to small  $t_{probe}$ , where the lineshape is broad and many details of the spectrum are lost. However, one can see the development of an elastic peak at short times with little spectrum in the gap. This corresponds to an excitation being created at the transition edge and immediately recombining by emitting a photon, without energy loss and time to break into spinons, yielding only an elastic signal at  $\omega = 0$ . On the other hand, if we allow the system to evolve under the action of the core-hole potential between absorption and emission, the resulting attractive force will bind the doublon to the core orbital and create spin domain walls (spinons), that will propagate throughout the system.

We also analyzed the effects the dipolar coupling  $\Gamma$  on the signal. In Fig. 7 we plot the spin-conserving and non-conserving contributions to the RIXS spectrum at fixed time  $t = 30$  and we observe that the lineshape broadens with increasing  $\Gamma$ , as expected. In addition we find that the magnitude of the signal grows, almost reaching perfect visibility, while the overall profile does not change much. One should notice that for large values of  $\Gamma$ , the dipolar term no longer acts as a small perturbation and affects the overall physical behavior of the system, with the photons becoming highly entangled with the conduction electrons. In that case, the numerical experiment no longer serves as a probe of the internal dynamics of the system.

## 2. Dependence on the core-hole potential

Finally, we observe that the magnitude of  $U_c$  affects the relative spectral weight between the high and low energy bands. This is demonstrated in Fig. 8, where we show the RIXS spectra obtained by varying  $U_c$  from 1.5 to 10. For large  $U_c$ , the core hole and a single doublon form a tightly bound state localized at the position of the core-orbital, effectively cutting the system in two. In the limit of  $U_c \rightarrow \infty$ , scattering with this potential induces holon-doublon excitations transferring weight into the upper Hubbard band, with a consequent increase in the spectral signal at high energies, while barely affecting the spectrum at low energies that originates from the spin degree of freedom.

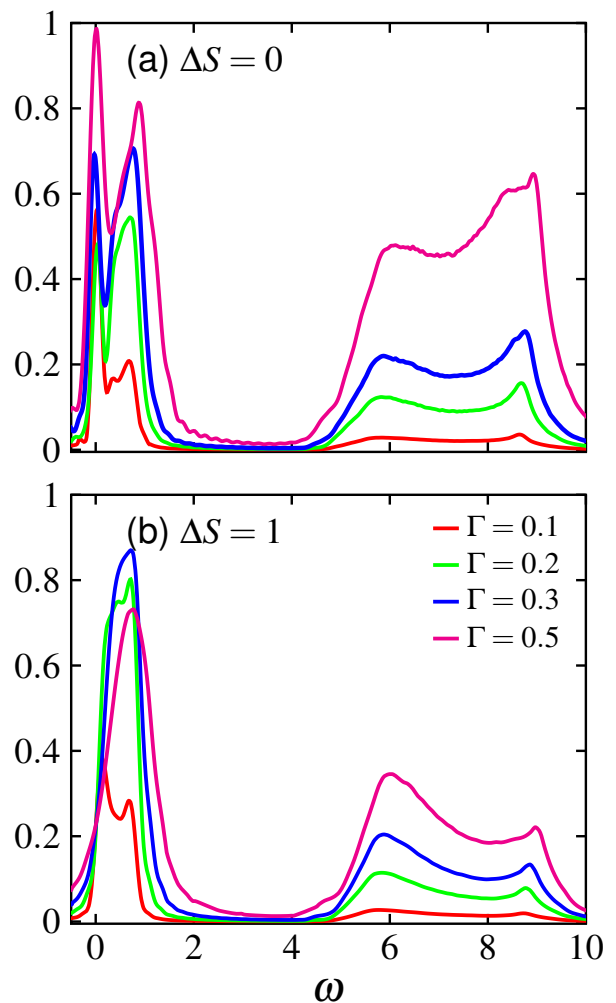


FIG. 7. (a) Spin conserving and (b) non-conserving RIXS channels for a Mott insulating Hubbard chain with  $U = 8$ ,  $U_c = 1.5$ ,  $L = 64$  sites, and different values of the dipolar coupling  $\Gamma$ .

## V. CONCLUSIONS

We have introduced a time-dependent scattering approach to core-hole spectroscopies that allows one to carry out numerical calculations without the full knowledge of the excitation spectrum of the system. The applicability of the method is demonstrated by means of time-dependent DMRG calculations. Results for the Hubbard model are achieved with minimal effort on large systems using a fraction of the states –and simulation time– required by the dynamical DMRG formulation. Unlike DDMRG and other approaches such as ED and DMFT that rely on explicitly calculating dynamical response functions, our time-dependent calculations are not limited by perturbation theory and contain contributions from higher order processes. In addition, our time-dependent approach can be readily applied without modification to non-equilibrium situations in which the



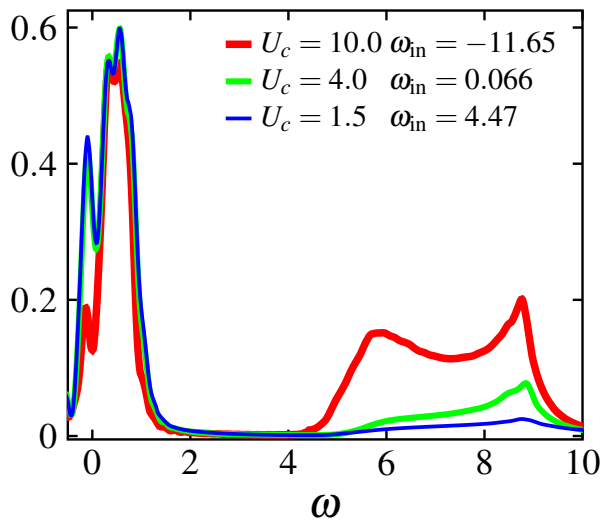


FIG. 8. RIXS results (without spin-orbit interaction) for a Mott insulating Hubbard chain with  $U = 8$ ,  $L = 64$  sites, and different values of the core-hole potential  $U_c$ .

electronic band is not in the ground state.

Our results show a remarkable departure from those obtained by means of ED, where the approach essentially consists of first calculating a spectrum corresponding to an infinite core-hole lifetime, and then convoluting this spectrum with a Lorentzian lifetime broadening. In our time-dependent simulations there is no way to control the internal dynamics of the system and the core-hole life-

time is basically determined by the probing time  $t_{probe}$ . At long times we always observe the emergence of low energy states that can be associated to gapless multi-spinon excitations. However, we observe that the spectral weight in the gap does decrease in the spin-conserving ( $\Delta S = 0$ ) channel when  $t_{probe}$  is reduced, consistent with the expectations from the UCL limit, that predict only an elastic signal at  $\omega = 0$ .

Our formulation can easily be implemented within other numerical frameworks, such as time-dependent DMFT. Momentum resolved calculations can be achieved by simple modifications of the described setup, although it requires one source and detector photon orbital per site. Work in this direction is currently underway.

## ACKNOWLEDGMENTS

We acknowledge generous computational resources provided by Northeastern University's Discovery Cluster at the Massachusetts Green High Performance Computing Center (MGHPCC). AN acknowledges the support from Compute Canada and the Advanced Research Computing at the University of British Columbia, where part of simulations were performed. AN is supported by the Canada First Research Excellence Fund. KZ is supported by a Faculty of the Future fellowship of the Schlumberger Foundation. AEF acknowledges the U.S. Department of Energy, Office of Basic Energy Sciences for support under grant No. DE-SC0014407.

- 
- [1] L. J. P. Ament, M. van Veenendaal, T. P. Devereaux, J. P. Hill, and J. van den Brink, *Rev. Mod. Phys.* **83**, 705 (2011).
  - [2] F. de Groot and A. Kotani, *Core Level Spectroscopy of Solids*, Advances in Condensed Matter Science (CRC Press, 2008).
  - [3] T. P. Devereaux and R. Hackl, *Rev. Mod. Phys.* **79**, 175 (2007).
  - [4] A. Kotani and S. Shin, *Rev. Mod. Phys.* **73**, 203 (2001).
  - [5] Y. Wang, M. Claassen, C. D. Pemmaraju, C. Jia, B. Moritz, and T. P. Devereaux, *Nature Reviews Materials* **3**, 312 (2018).
  - [6] J.-P. Rueff and A. Shukla, *Journal of Electron Spectroscopy and Related Phenomena* **188**, 10 (2013), progress in Resonant Inelastic X-Ray Scattering.
  - [7] F. De Groot, *Chemical Reviews* **101**, 1779 (2001).
  - [8] J. Rehr, *Radiation Physics and Chemistry* **75**, 1547 (2006), proceedings of the 20th International Conference on X-ray and Inner-Shell Processes.
  - [9] Y. Chen, Y. Wang, C. Jia, B. Moritz, A. M. Shvaika, J. K. Freericks, and T. P. Devereaux, *Phys. Rev. B* **99**, 104306 (2019).
  - [10] C. Jia, K. Wohlfeld, Y. Wang, B. Moritz, and T. P. Devereaux, *Phys. Rev. X* **6**, 021020 (2016).
  - [11] K. Tsutsui, T. Tohyama, and S. Maekawa, *Phys. Rev. B* **61**, 7180 (2000).
  - [12] S. Kourtis, J. van den Brink, and M. Daghofer, *Phys. Rev. B* **85**, 064423 (2012).
  - [13] U. Kumar, A. Nocera, E. Dagotto, and S. Johnston, *New Journal of Physics* **20**, 073019 (2018).
  - [14] U. Kumar, A. Nocera, E. Dagotto, and S. Johnston, *Phys. Rev. B* **99**, 205130 (2019).
  - [15] Y. Wang, Y. Chen, C. Jia, B. Moritz, and T. P. Devereaux, arXiv preprint arXiv:1905.05405 (2019).
  - [16] L. Braicovich, J. van den Brink, V. Bisogni, M. M. Sala, L. J. P. Ament, N. B. Brookes, G. M. De Luca, M. Saluzzo, T. Schmitt, V. N. Strocov, and G. Ghiringhelli, *Phys. Rev. Lett.* **104**, 077002 (2010).
  - [17] M. Le Tacon, G. Ghiringhelli, J. Chaloupka, M. M. Sala, V. Hinkov, M. Haverkort, M. Minola, M. Bakr, K. Zhou, S. Blanco-Canosa, *et al.*, *Nature Physics* **7**, 725 (2011).
  - [18] M. Dean, *Journal of Magnetism and Magnetic Materials* **376**, 3 (2015), pseudogap, Superconductivity and Magnetism.
  - [19] H. Suzuki, M. Minola, Y. Lu, Y. Peng, R. Fumagalli, E. Lefrançois, T. Loew, J. Porras, K. Kummer, D. Betto, *et al.*, *npj Quantum Materials* **3**, 65 (2018).
  - [20] R. S. Markiewicz, T. Das, and A. Bansil, *Phys. Rev. B* **82**, 224501 (2010).
  - [21] A. Klauser, J. Mossel, J.-S. Caux, and J. van den Brink, *Phys. Rev. Lett.* **106**, 157205 (2011).

- [22] M. W. Haverkort, G. Sangiovanni, P. Hansmann, A. Toschi, Y. Lu, and S. Macke, *EPL (Europhysics Letters)* **108**, 57004 (2014).
- [23] W. S. Lee, S. Johnston, B. Moritz, J. Lee, M. Yi, K. J. Zhou, T. Schmitt, L. Patthey, V. Strocov, K. Kudo, Y. Koike, J. van den Brink, T. P. Devereaux, and Z. X. Shen, *Phys. Rev. Lett.* **110**, 265502 (2013).
- [24] K. Okada and A. Kotani, *Phys. Rev. B* **63**, 045103 (2001).
- [25] C. Jia, E. Nowadnick, K. Wohlfeld, Y. Kung, C.-C. Chen, S. Johnston, T. Tohyama, B. Moritz, and T. Devereaux, *Nat. Commun.* **5** (2014).
- [26] C. Monney, V. Bisogni, K.-J. Zhou, R. Kraus, V. N. Strocov, G. Behr, J. c. v. Málek, R. Kuzian, S.-L. Drechsler, S. Johnston, A. Revcolevschi, B. Büchner, H. M. Rønnow, J. van den Brink, J. Geck, and T. Schmitt, *Phys. Rev. Lett.* **110**, 087403 (2013).
- [27] S. Johnston, C. Monney, V. Bisogni, K.-J. Zhou, R. Kraus, G. Behr, V. N. Strocov, J. Málek, S.-L. Drechsler, J. Geck, T. Schmitt, and J. van den Brink, *Nature Commun.* **7**, 10563 (2016).
- [28] F. Vernay, B. Moritz, I. S. Elfimov, J. Geck, D. Hawthorn, T. P. Devereaux, and G. A. Sawatzky, *Phys. Rev. B* **77**, 104519 (2008).
- [29] C.-C. Chen, B. Moritz, F. Vernay, J. N. Hancock, S. Johnston, C. J. Jia, G. Chabot-Couture, M. Greven, I. Elfimov, G. A. Sawatzky, and T. P. Devereaux, *Phys. Rev. Lett.* **105**, 177401 (2010).
- [30] K. Okada and A. Kotani, *J. Phys. Soc. Jpn.* **75**, 044702 (2006).
- [31] R. O. Kuzian, S. Nishimoto, S.-L. Drechsler, J. Málek, S. Johnston, J. van den Brink, M. Schmitt, H. Rosner, M. Matsuda, K. Oka, H. Yamaguchi, and T. Ito, *Phys. Rev. Lett.* **109**, 117207 (2012).
- [32] K. Tsutsui and T. Tohyama, *Phys. Rev. B* **94**, 085144 (2016).
- [33] T. Tohyama, K. Tsutsui, M. Mori, S. Sota, and S. Yunoki, *Phys. Rev. B* **92**, 014515 (2015).
- [34] K. Ishii, K. Tsutsui, Y. Endoh, T. Tohyama, S. Maekawa, M. Hoesch, K. Kuzushita, M. Tsubota, T. Inami, J. Mizuki, Y. Murakami, and K. Yamada, *Phys. Rev. Lett.* **94**, 207003 (2005).
- [35] K. Tsutsui, T. Tohyama, and S. Maekawa, *Phys. Rev. Lett.* **91**, 117001 (2003).
- [36] M. A. van Veenendaal and G. A. Sawatzky, *Phys. Rev. B* **49**, 3473 (1994).
- [37] C. Jia, C. Chen, A. Sorini, B. Moritz, and T. Devereaux, *New Journal of Physics* **14**, 113038 (2012).
- [38] A. Nocera, U. Kumar, N. Kaushal, G. Alvarez, E. Dagotto, and S. Johnston, *Scientific Reports* **8**, 11080 (2018).
- [39] A. Nocera and G. Alvarez, *Phys. Rev. E* **94**, 053308 (2016).
- [40] E. Jeckelmann, *Phys. Rev. B* **66**, 045114 (2002).
- [41] T. D. Kühner and S. R. White, *Phys. Rev. B* **60**, 335 (1999).
- [42] J. Schlappa, K. Wohlfeld, K. Zhou, M. Mourigal, M. Haverkort, V. Strocov, L. Hozoi, C. Monney, S. Nishimoto, S. Singh, *et al.*, *Nature* **485**, 82 (2012).
- [43] A. S. Landsman and U. Keller, *Physics Reports* **547**, 1 (2015), attosecond science and the tunneling time problem.
- [44] S. R. White and A. E. Feiguin, *Phys. Rev. Lett.* **93**, 076401 (2004).
- [45] A. J. Daley, C. Kollath, U. Schollwöck, and G. Vidal, *Journal of Statistical Mechanics: Theory and Experiment* **2004**, P04005 (2004).
- [46] A. E. Feiguin, in *XV Training Course in the Physics of Strongly Correlated Systems*, Vol. 1419 (AIP Proceedings, 2011) p. 5.
- [47] S. Paeckel, T. Khler, A. Swoboda, S. R. Manmana, U. Schollwöck, and C. Hubig, *Annals of Physics* **411**, 167998 (2019).
- [48] L. J. P. Ament, F. Forte, and J. van den Brink, *Phys. Rev. B* **75**, 115118 (2007).
- [49] A. E. Feiguin and D. A. Huse, *Phys. Rev. B* **79**, 100507 (2009).
- [50] K. A. Al-Hassanieh, F. A. Reboredo, A. E. Feiguin, I. González, and E. Dagotto, *Phys. Rev. Lett.* **100**, 166403 (2008).
- [51] L. G. G. V. Dias da Silva, K. A. Al-Hassanieh, A. E. Feiguin, F. A. Reboredo, and E. Dagotto, *Phys. Rev. B* **81**, 125113 (2010).
- [52] J. Rincón, K. A. Al-Hassanieh, A. E. Feiguin, and E. Dagotto, *Phys. Rev. B* **90**, 155112 (2014).
- [53] R. Sensarma, D. Pekker, E. Altman, E. Demler, N. Strohmaier, D. Greif, R. Jördens, L. Tarruell, H. Moritz, and T. Esslinger, *Phys. Rev. B* **82**, 224302 (2010).
- [54] M. Eckstein and P. Werner, *Phys. Rev. B* **84**, 035122 (2011).
- [55] Z. Lenarčič and P. Prelovšek, *Phys. Rev. Lett.* **111**, 016401 (2013).
- [56] M. Eckstein and P. Werner, *Scientific Reports* **6**, 21235 EP (2016), article L3 -.